AIP Applied Physics Letters

Controlling a microdisk laser by local refractive index perturbation

Seng Fatt Liew, Li Ge, Brandon Redding, Glenn S. Solomon, and Hui Cao

Citation: Applied Physics Letters **108**, 051105 (2016); doi: 10.1063/1.4940229
View online: http://dx.doi.org/10.1063/1.4940229
View Table of Contents: http://scitation.aip.org/content/aip/journal/apl/108/5?ver=pdfcov
Published by the AIP Publishing

Articles you may be interested in
Active control of emission directionality of semiconductor microdisk lasers
Appl. Phys. Lett. **104**, 231108 (2014); 10.1063/1.4883637

Lasing properties of non-polar GaN quantum dots in cubic aluminum nitride microdisk cavities
Appl. Phys. Lett. **103**, 021107 (2013); 10.1063/1.4813408

Compact microdisk cavity laser with type-II GaSb/GaAs quantum dots
Appl. Phys. Lett. **98**, 051105 (2011); 10.1063/1.3543839

Small optical volume terahertz emitting microdisk quantum cascade lasers
Appl. Phys. Lett. **90**, 141114 (2007); 10.1063/1.2719674

CdSe quantum dot microdisk laser
Appl. Phys. Lett. **89**, 231104 (2006); 10.1063/1.2402263

Reuse of AIP Publishing content is subject to the terms at: https://publishing.aip.org/authors/rights-and-permissions. IP: 130.132.173.84 On: Fri, 05 Feb 2016 20:30:23

APPLIED PHYSICS LETTERS **108**, 051105 (2016)

Controlling a microdisk laser by local refractive index perturbation

Seng Fatt Liew,[1] Li Ge,[2,3] Brandon Redding,[1] Glenn S. Solomon,[4] and Hui Cao[1,a)]
[1]*Department of Applied Physics, Yale University, New Haven, Connecticut 06520, USA*
[2]*Department of Engineering Science and Physics, College of Staten Island, CUNY, Staten Island, New York 10314, USA*
[3]*The Graduate Center, CUNY, New York, New York 10016, USA*
[4]*Joint Quantum Institute, NIST and University of Maryland, Gaithersburg, Maryland 20899, USA*

(Received 12 October 2015; accepted 7 January 2016; published online 3 February 2016)

We demonstrate a simple yet effective approach of controlling lasing in a semiconductor microdisk by photo-thermal effect. A continuous wave green laser beam, focused onto the microdisk perimeter, can enhance or suppress lasing in different cavity modes, depending on the position of the focused beam. Its main effect is a local modification of the refractive index of the disk, which results in an increase in the power slope of some lasing modes and a decrease of others. The boundary roughness breaks the rotational symmetry of a circular disk, allowing the lasing process to be tuned by varying the green beam position. Using the same approach, we can also fine tune the relative intensity of a quasi-degenerate pair of lasing modes. Such post-fabrication control, enabled by an additional laser beam, is flexible and reversible, thus enhancing the functionality of semiconductor microdisk lasers. © *2016 AIP Publishing LLC*. [http://dx.doi.org/10.1063/1.4940229]

Semiconductor microdisk lasers have simple geometries, small footprints, and low lasing thresholds, making them attractive on-chip light sources for integrated photonics applications.[1,2] Due to high refractive index contrast at the disk boundary, light is strongly confined by total internal reflection, forming whispering-gallery modes (WGMs) with high-quality (Q) factors. A circular microdisk of size much larger than the optical wavelength supports densely packed WGMs, and lasing usually occurs in multiple modes at different frequencies. Post-fabrication tuning of these modes' frequencies, lasing thresholds, and emission intensities are desired for many applications.

Over the years, various methods have been developed to control semiconductor microcavity lasers. For example, it has been shown that the lasing frequency can be tuned by changing the refractive index of the cavity *via* thermal effects,[3,4] oxidation,[5–7] a chemical process,[8] the photochromic effect,[9] or using a liquid crystal,[10] microfluidics,[11,12] a chalcogenide glass,[13] a mechanical perturbation,[14] and an ultrafast laser.[15] Among these schemes, refractive index change induced by a photo-thermal effect is reversible, easy to realize, and cost-effective. The laser-induced thermal effect can be confined to a small region if the thermal conductivity of the surrounding medium is sufficiently high to allow fast thermal exchange.[16] Therefore, laser heating can cause localized and selective perturbation to the semiconductor microcavity by changing the local refractive index.

A different approach employs pump engineering to switch the lasing mode from one cavity resonance to another. The lasing threshold of the target mode is reduced by enhancing its spatial overlap with the pump pattern.[17–26] Even without prior knowledge of the spatial profiles of the cavity resonances, selective pumping of the lasing modes can still be achieved by employing optimization algorithms.[27–31] However, such a method is inherently slow because it relies on a feedback mechanism to find the optimal pump pattern.

Here, we demonstrate a simpler method based on the photo-thermal effect to control lasing in a GaAs microdisk. Most of the previous works using a laser-induced thermal effect aimed to tune the resonance frequencies in photonic crystal cavities (see, for example, Refs. 3, 4, and 16). In this work, we show that by focusing a continuous wave (CW) laser beam on a microdisk boundary, the photo-thermal effect can either enhance or suppress lasing in different modes, depending on the position of the focused beam. The boundary roughness breaks the rotational symmetry of the nominal circular disk, allowing the lasing process to be tuned by varying the green beam position. The emission intensities of some lasing modes increase when illuminated by an additional laser beam despite the increase of the disk temperature. This is the opposite of the typical behavior of semiconductor quantum dot (QD) lasers at elevated temperature, and it is attributed to the nonlinear interactions of the lasing modes. Using the same approach, we also modulate the relative intensities of two quasi-degenerate lasing modes. Our numerical simulation illustrates that such changes are caused by the differential modification of the quality (Q) factors of the quasi-degenerate modes as a result of local refractive index change.

The microdisk is fabricated on a GaAs wafer following the procedure described in Ref. 31. Figure 1 shows the scanning electron microscope (SEM) images of a fabricated disk. From the top-view SEM image [Fig. 1(a)], the disk shape is very close to a circle, and the disk radius is $R = 9.2\,\mu$m. The high-magnification tilt-view SEM image [Fig. 1(b)] reveals the roughness of the disk sidewall created during the etching process. The fabricated microdisks are mounted in a low-temperature cryostat for the lasing experiment. The experimental setup is similar to the one described in Ref. 30 except that we added an additional CW green laser ($\lambda = 532$ nm) to introduce a local refractive index change by the photo-thermal effect. The InAs QDs were optically excited by a mode-

a)hui.cao@yale.edu

 © 2016 AIP Publishing LLC

Reuse of AIP Publishing content is subject to the terms at: https://publishing.aip.org/authors/rights-and-permissions. IP: 130.132.173.84 On: Fri, 05 Feb 2016 20:30:23

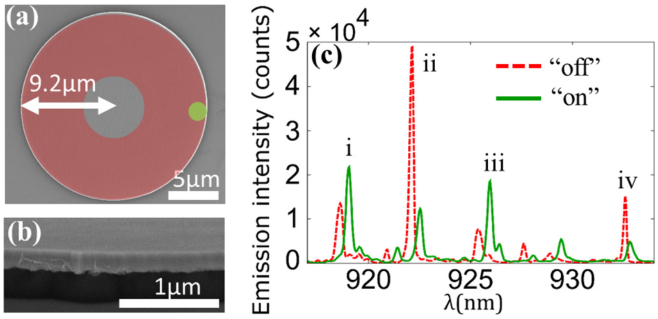

FIG. 1. (a) Top-view scanning electron microscope (SEM) image of a fabricated GaAs microdisk, showing an almost circular shape of the disk. The microdisk, with InAs quantum dots embedded inside, is optically pumped by a mode-locked Ti:Sapphire laser with a uniform ring pattern (red ring) and perturbed locally by an additional green laser beam (green circle). (b) Magnified tilt-view SEM image of the microdisk, revealing the sidewall roughness. (c) Emission spectra showing multiple lasing peaks when the green laser beam is off (dashed red line) and all the peaks are red-shifted when it is on (solid green line). Intensities of lasing modes i and iii increase, while those of modes ii and iv decrease, when the green laser beam is on.

locked Ti:Sapphire laser ($\lambda_p = 790$ nm, 76 MHz repetition rate, 200 fs pulses). As shown schematically in Fig. 1(a), we shaped the pump pattern of the Ti:Sapphire laser to a uniform ring because the high-Q modes have little overlap with the central region of the disk, where light could leak to the substrate via the pedestal. Many modes lased simultaneously as seen in the emission spectrum Fig. 1(c) and below we focus on four dominant lasing modes labeled i-iv.

Since all the high-Q modes have maximum field intensity near the disk's boundary, they would experience the most perturbation when a green laser beam is focused to the disk edge to induce local refractive index change [Fig. 1(a)]. The focused green beam has a Gaussian spatial profile with a full-width at half-maximum (FWHM) of about 1.8 μm. Figure 1(c) shows the lasing spectrum when the incident power of the green laser at the focus is 1.6 mW. Once the green beam is on, all lasing peaks are red-shifted in frequency. The magnitude of the frequency shift depends on the green laser power, and it is roughly 0.2 nm/mW. In addition to the change in lasing frequency, the emission intensities of modes i and iii increase while those of modes ii and iv decrease [Fig. 1(c)]. This process is reversible, the lasing spectrum changed back to the original one after the green laser was switched off.

There are two processes induced by the green laser. One is a non-reversible photo-induced oxidation of GaAs, which reduces the refractive index of the disk and blue-shifts the cavity resonances.[6] The other is a reversible photo-thermal effect, which increases the refractive index of the disk *via* heating, and red-shifts the lasing modes.[3,32] Since we observe a red-shift of the lasing modes and the process is reversible, we conclude that the photo-thermal effect dominates over the oxidation process. Moreover, the sample is mounted in a vacuum chamber in which the oxidation process is unlikely to occur due to insufficient oxygen supply. Experimentally we do not observe lasing or amplification of spontaneous emission in the microdisk when only the green laser is turned on and the red pump laser is switched off, suggesting the dominant effect of the green light on the mirodisk laser is a modification of the refractive index of the disk *via* the photo-thermal effect. To confirm this postulation, we calculate the refractive index change from the GaAs thermal properties[33–35] and temperature distribution induced by the focused green laser beam.[16] The estimated lasing wavelength shift is 0.3 nm/mW, comparable to the 0.2 nm/mW observed experimentally.

Typically, the laser-induced heating weakens the confinement of carriers in the QDs, reducing the optical gain. Thus, the emission intensity is expected to decrease for all modes. However, some lasing modes have stronger emission when the green laser is on. To further characterize the change of the lasing modes, we measured the emission intensity of each mode as a function of the red pump power, P with the green laser on or off. Figure 2(a) shows the data for mode ii, whose intensity decreases significantly with the green light on. In the absence of the green laser beam, mode ii displays a sharp increase in the growth rate of its intensity with pump at $P \sim 3$ mW, indicating the onset of lasing action. With the green beam on, mode ii starts lasing at slightly higher P, but its emission intensity grows at a significantly reduced rate above the lasing threshold. Thus, the local perturbation introduced by the green light affects mostly the power slope of the lasing mode. Opposite of the behavior of mode ii, when the green beam is on, the intensity of mode iii grows faster after it lases, even though its lasing threshold also increases slightly [Fig. 2(b)].

To be more quantitative, we extract the lasing threshold and power slope of individual lasing modes from the dependence of their emission intensity on the pump power [Figs. 2(c) and 2(d)]. Without the green light, mode iii is the first to lase but the lasing thresholds of other modes differ only by a few percent. All the lasing modes experience an increase of lasing threshold with the green beam on, but the order of lasing remains the same. Opposite of the overall

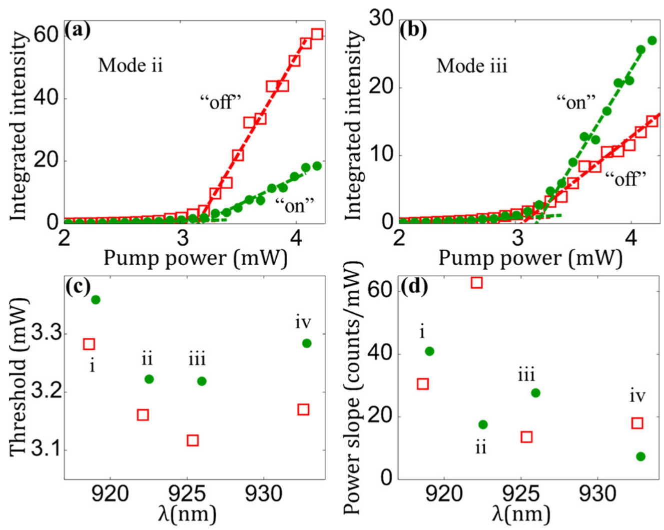

FIG. 2. Measured emission intensities of mode ii (a) and mode iii (b) as a function of the incident red pump power when the green beam is switched off (open red squares) and on (solid green circles). Comparison of the thresholds (c) and power slopes (d) of the major lasing modes i–iv shown in Fig. 1, when the green beam is off (open red squares) and on (solid green circles). The lasing threshold increase of all modes is attributed to the reduced carrier confinement in the QDs at the elevated temperature. The power slopes for modes ii and iv decrease, while the power slopes for modes i and iii increase with the green beam on.

Reuse of AIP Publishing content is subject to the terms at: https://publishing.aip.org/authors/rights-and-permissions. IP: 130.132.173.84 On: Fri, 05 Feb 2016 20:30:23

increment of lasing threshold in Fig. 2(c), the power slope exhibits a different behavior in the presence of the green light [Fig. 2(d)]. In particular, the power slopes of modes i and iii increase while those of modes ii and iv decrease. The opposite change in the power slope is attributed to the nonlinear interaction of the lasing modes, which is modified by the green laser beam. The power slope of one lasing mode depends not only on its own lasing threshold but also on the intensities of other lasing modes. The photo-thermal effect induces a local refractive index change, which modifies the quality (Q) factors of cavity resonances. The increase of the power slope for the first lasing mode (mode iii) and the decrease of the power slope for the second lasing mode (mode ii) can be predicted by the Steady-state *Ab-initio* Laser Theory (SALT),[37,38] when the Q of mode ii is reduced more than mode iii by the local refractive index change. In other words, the increase of power slope for mode iii is due to reduced gain competition from mode ii which lases less efficiently as a result of stronger Q spoiling. Thus, the perturbation introduced by the green beam is not always detrimental to the lasing action, and it provides a simpler method to switch the dominant lasing mode from one to another.

The presence of sidewall roughness breaks the rotational symmetry of the microdisk, making the photo-thermal effect on the lasing modes depend on the position of the focused green laser beam. Next, we investigate the change of lasing modes when the focused green beam is moved along the disk boundary [Fig. 3(a)]. While the spot size of the green beam is 1.8 μm, the heat it generates spreads to a larger area. Experimentally, we observe a notable variation of the lasing spectra when the azimuthal angle θ of the green spot is changed by 36°, which corresponds to an arc length of 5.8 μm. Figure 3(b) shows the lasing spectra as the green beam spot is moved azimuthally across the perimeter of the disk. Individual lasing modes change in different ways, for example, the intensity of mode ii first increases and reaches the maximum at $\theta = 72°$, then it decreases and reaches the minimum at about $\theta = 180°$ before rising again. Mode iv displays a more dramatic change, its lasing is turned off at $\theta = 180°$. In contrast to modes ii and iv, mode iii has the maximal emission at about $\theta = 180°$.

In the following, we take a closer look at the lasing mode iii, whose line shape also changes with the position of the green beam. Figures 3(c) and 3(d) show the spectral line of mode iii when the green beam spot is at $\theta = 0°$ and 180°, respectively. At $\theta = 0°$, the line shape differs from a symmetric Lorentzian curve, indicating the peak consists of two sub-peaks. The whispering-gallery modes in a perfect circular disk are degenerate, however, due to the roughness of the disk sidewall, the frequency degeneracy is lifted and the quasi-degenerate modes are formed. We decompose the spectral line to recover the two quasi-degenerate modes L_1 and L_2, and also include an additional peak L_3 from a nearby resonance that has significantly weaker emission. At $\theta = 0°$ [Fig. 3(c)], the two quasi-degenerate modes L_1 and L_2 have similar emission intensity; but at $\theta = 180°$ only one of the quasi-degenerate modes, L_1, lases, and the spectral line becomes narrower and symmetric [Fig. 3(d)].

Figure 3(e) plots the intensities of the two quasi-degenerate modes, L_1, L_2, as a function of the position of the

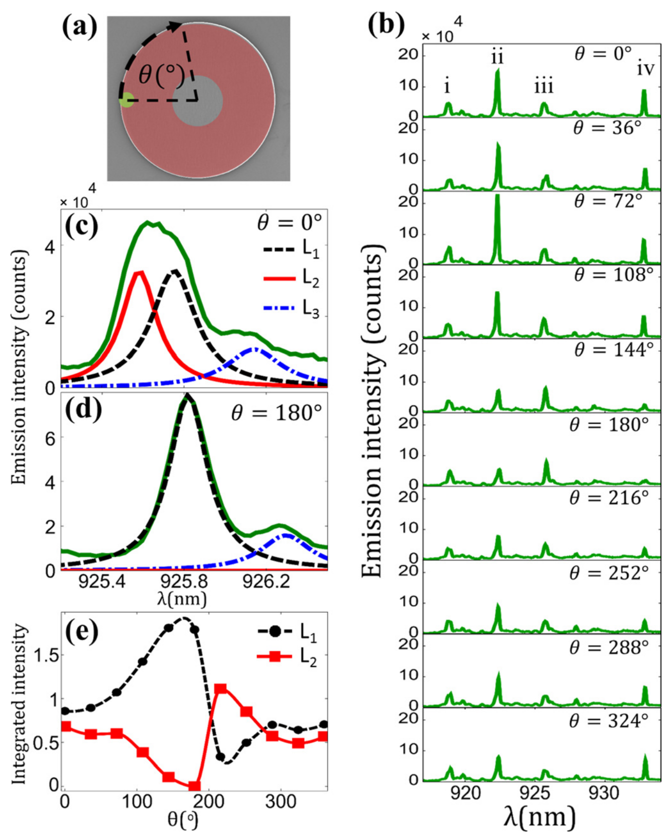

FIG. 3. (a) The green laser beam is focused to a 1.8 μm spot and moved azimuthally along the microdisk's perimeter. Its power is fixed at 1.4 mW. (b) Measured emission spectra with the green spot at different locations indicated by the azimuthal angle θ. (c) and (d) Spectral line of lasing mode iii (solid green line) when the green beam spot is at $\theta = 0°$ (c) and 180° (d). The spectrum is decomposed by three Lorentzian lines, two of them (L_1 and L_2) compose the lasing peak iii and a third one (L_3) for a nearby resonance of lower intensity. (e) The emission intensities of the two quasi-degenerate modes L_1 and L_2 as a function of the green laser beam's location at the disk's boundary. L_1 and L_2 have comparable intensity at θ close to 0°, but their intensities differ significantly when θ approaches 180°.

green beam θ. While L_1 and L_2 have similar intensity at $\theta = 0°$, L_1 is enhanced and L_2 is suppressed as the green spot moves towards 180°. Their difference becomes the largest at $\theta \approx 180°$, where L_2 nearly disappears and L_1 has the maximal intensity. With a further increase of θ beyond 180°, L_1 goes down while L_2 grows, eventually L_2 becomes stronger than L_1. Their difference diminishes as θ approaches 360°. In contrast to the drastic change of L_1 and L_2, L_3 exhibits only slight fluctuation of its intensity around the mean value (not shown), when the green spot moves to different locations. This result shows that by focusing the green laser beam onto different locations, we can tune the relative intensity of the quasi-degenerate modes and even switch off lasing in one of them.

Given that the quasi-degenerate modes have a similar spatial field profile, it is surprising that the focused green laser beam, whose spot size is much larger than the wavelength, can induce a different response from them. To understand such phenomena, we perform a numerical simulation on a 2D dielectric disk without gain or loss. Random harmonic perturbations are added to the disk boundary to emulate the sidewall roughness on the fabricated disk. To reduce the computing time, we set the disk radius to be $R = 3\,\mu$m,

Reuse of AIP Publishing content is subject to the terms at: https://publishing.aip.org/authors/rights-and-permissions. IP: 130.132.173.84 On: Fri, 05 Feb 2016 20:30:23

smaller than the measured one. The effective index of refraction of the disk is computed from the thickness of the fabricated disk, and its value is $n = 3.13$.[36] As mentioned earlier, the dominant effect of the green laser beam is an increase of the local refractive index of the disk *via* the photo-thermal effect. To match the ratio of the green beam spot size to the microdisk dimension in the experiment, we increase the refractive index of the disk within a circular region of diameter $d = 600$ nm in the simulation. Based on the experimentally observed wavelength shift $\delta\lambda$ of the lasing peaks, we set the change of refractive index to be $\delta n = (\delta\lambda/\lambda)(2\pi R/d) \simeq 0.01$. We calculate the resonant modes of the passive microdisk using the finite-difference frequency-domain (FDFD) method with and without the perturbation of the green light. Figure 4(a) shows the spatial field distribution for one pair of high-Q quasi-degenerate modes in the absence of the perturbation. Although their spatial field profiles look very similar, their Q factors and center wavelengths λ are slightly different due to the roughness of the disk boundary. The perturbation of the green beam causes further changes in Q and λ. As shown in Figs. 4(b) and 4(c), with the green beam focused on different locations on the disk, the Q values of the quasi-degenerate modes 1 and 2 can either approach each other or move further apart. Next we introduce optical gain to the microdisk, and compute the lasing intensity as a function of the pump strength using the SALT.[37,38] Figure 4(d) plots the emission intensities of modes 1 and 2, when the "green beam spot" is at two spatial locations shown in Fig. 4(b). Their intensities get closer when the difference in their Q's is reduced by the green beam. However, when the green beam is moved to another location, the Q difference is increased, and so is the intensity. The numerical results, which agree qualitatively with the experimental data, illustrate the sensitivity of quasi-degenerate lasing modes to the spatial-dependent perturbation of the green laser beam.

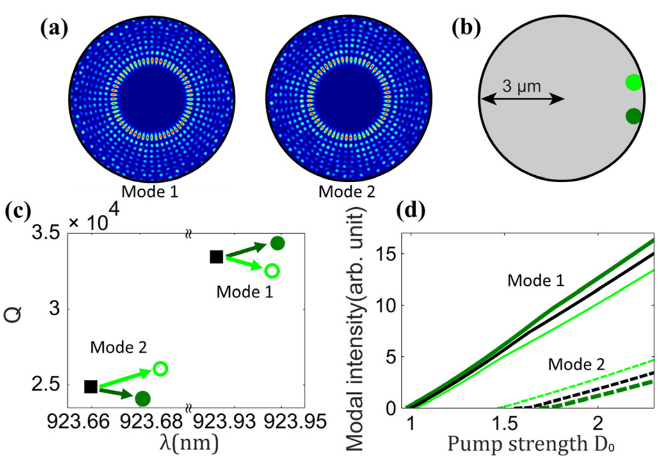

FIG. 4. (a) Calculated spatial field distributions of two quasi-degenerate modes in a passive microdisk of radius 3 μm. (b) Schematic diagram of local perturbation of the disk by the green beam. (c) Center wavelength, λ, and quality factor, Q, of the quasi-degenerate modes shown in (a) without the green beam (black solid squares) and with the green beam at two spatial locations (dark green solid circles, light green open circles) that are marked in (b). (d) Calculated intensities of the two modes as a function of the pump strength without the green beam (black lines) and with the green beam at two spatial locations (dark green lines, light green lines) marked in (b).

In conclusion, we demonstrate a simple yet effective method to control the lasing modes in a semiconductor microdisk using an additional laser beam at a different wavelength. By moving the beam spot on the disk, we can either enhance or suppress lasing in individual modes by modifying the power slope. Different lasing modes display a distinct or even opposite response to the perturbation of the additional laser beam, allowing us to switch the dominant lasing mode. Moreover, we can tune the relative intensity of the quasi-degenerate lasing modes. All the changes induced by the additional laser beam, which is a low-power continuous wave, are reversible. The microdisk boundary roughness is essential to controlling the lasing process by varying the green beam position, which would otherwise be impossible for a perfectly circular microdisk. Such post-fabrication tuning of lasing modes is flexible and sensitive, thus enhancing the functionality of semiconductor microdisk lasers.

This work was supported by the MURI Grant No. N00014-13-1-0649 from the U.S. Office of Naval Research and by the National Science Foundation under the Grant Nos. DMR-1205307 and DMR-1506987. Facilities use was supported by YINQE and NSF MRSEC DMR-1119826.

[1]S. L. McCall, A. F. J. Levi, R. E. Slusher, S. J. Pearton, and R. A. Logan, Appl. Phys. Lett. **60**, 289 (1992).
[2]M. Fujita, A. Sakai, and T. Baba, IEEE J. Sel. Top. Quantum Electron. **5**, 673 (1999).
[3]A. Faraon, D. Englund, I. Fushman, and J. Vučković, Appl. Phys. Lett. **90**, 213110 (2007).
[4]A. Faraon and J. Vučković, Appl. Phys. Lett. **95**, 043102 (2009).
[5]K. Hennessy, C. Högerle, E. Hu, A. Badolato, and A. Imamoğlu, Appl. Phys. Lett. **89**, 041118 (2006).
[6]H. S. Lee, S. Kiravittaya, S. Kumar, J. D. Plumhof, L. Balet, L. H. Li, M. Francardi, A. Gerardino, A. Fiore, A. Rastelli, and O. G. Schmidt, Appl. Phys. Lett. **95**, 191109 (2009).
[7]F. Intonti, N. Caselli, S. Vignolini, F. Riboli, L. Balet, L. H. Li, M. Francardi, A. Gerardino, A. Fiore, and M. Gurioli, Appl. Phys. Lett. **100**, 033116 (2012).
[8]K. Hennessy, A. Badolato, A. Tamboli, P. M. Petroff, E. Hu, M. Atatüre, J. Dreiser, and A. Imamoğlu, Appl. Phys. Lett. **87**, 021108 (2005).
[9]D. Sridharan, E. Waks, G. Solomon, and J. T. Fourkas, Appl. Phys. Lett. **96**, 153303 (2010).
[10]B. Maune, M. Lončar, J. Witzens, M. Hochberg, T. B. Jones, D. Psaltis, and A. Scherer, Appl. Phys. Lett. **85**, 360 (2004).
[11]D. Erickson, T. Rockwood, T. Emery, A. Scherer, and D. Psaltis, Opt. Lett. **31**, 59 (2006).
[12]F. Intonti, S. Vignolini, V. Törck, M. Colocci, P. Bettotti, L. Pavesi, S. L. Schweizer, R. Wehrspohn, and D. Wiersma, Appl. Phys. Lett. **89**, 211117 (2006).
[13]A. Faraon, D. Englund, D. Bulla, B. Luther-Davies, B. J. Eggleton, N. Stoltz, P. Petroff, and J. Vučković, Appl. Phys. Lett. **92**, 043123 (2008).
[14]Y. Gong, B. Ellis, G. Shambat, T. Sarmiento, J. S. Harris, and J. Vučković, Opt. Express **18**, 8781 (2010).
[15]R. Bruck, B. Mills, B. Troia, D. J. Thomson, F. Y. Gardes, Y. Hu, G. Z. Mashanovich, V. M. N. Passaro, G. T. Reed, and O. L. Muskens, Nat. Photonics **9**, 54 (2015).
[16]S. Sokolov, J. Lian, E. Yüce, S. Combrié, G. Lehoucq, A. De Rossi, and A. P. Mosk, Appl. Phys. Lett. **106**, 171113 (2015).
[17]S. F. Pereira, M. B. Willemsen, M. P. van Exter, and J. P. Woerdman, Appl. Phys. Lett. **73**, 2239 (1998).
[18]Y. F. Chen and Y. P. Lan, J. Opt. B **3**, 146 (2001).
[19]Y. F. Chen, Y. P. Lan, and S. C. Wang, Appl. Phys. B **72**, 167 (2001).
[20]J.-F. Bisson, A. Shirakawa, Y. Sato, Y. Senatsky, and K.-I. Ueda, Opt. Rev. **11**, 353 (2004).
[21]D. Naidoo, T. Godin, M. Fromager, E. Cagniot, N. Passilly, A. Forbes, and K. At-Ameur, Opt. Commun. **284**, 5475 (2011).
[22]N. B. Rex, R. K. Chang, and L. J. Guido, IEEE Photonics Technol. Lett. **13**, 1 (2001).

Reuse of AIP Publishing content is subject to the terms at: https://publishing.aip.org/authors/rights-and-permissions. IP: 130.132.173.84 On: Fri, 05 Feb 2016 20:30:23

[23] G. D. Chern, H. E. Tureci, A. D. Stone, R. K. Chang, M. Kneissl, and N. M. Johnson, Appl. Phys. Lett. **83**, 1710 (2003).
[24] T. Fukushima, T. Harayama, P. Davis, P. O. Vaccaro, T. Nishimura, and T. Aida, Opt. Lett. **27**, 1430 (2002).
[25] M. Kneissl, M. Teepe, N. Miyashita, N. M. Johnson, G. D. Chern, and R. K. Chang, Appl. Phys. Lett. **84**, 2485 (2004).
[26] S. Shinohara, T. Harayama, T. Fukushima, M. Hentschel, T. Sasaki, and E. E. Narimanov, Phys. Rev. Lett. **104**, 163902 (2010).
[27] M. Leonetti and C. Lopez, Appl. Phys. Lett. **102**, 071105 (2013).
[28] N. Bachelard, J. Andreasen, S. Gigan, and P. Sebbah, Phys. Rev. Lett. **109**, 033903 (2012).
[29] N. Bachelard, S. Gigan, X. Noblin, and P. Sebbah, Nat. Phys. **10**, 426 (2014).
[30] S. F. Liew, B. Redding, L. Ge, G. S. Solomon, and H. Cao, Appl. Phys. Lett. **104**, 231108 (2014).
[31] S. F. Liew, L. Ge, B. Redding, G. S. Solomon, and H. Cao, Phys. Rev. A **91**, 043828 (2015).
[32] A. Kiraz, P. Michler, C. Becher, B. Gayral, A. Imamoğlu, L. Zhang, E. Hu, W. V. Schoenfeld, and P. M. Petroff, Appl. Phys. Lett. **78**, 3932 (2001).
[33] D. E. Aspnes, S. M. Kelso, R. A. Logan, and R. Bhat, J. Appl. Phys. **60**, 754 (1986).
[34] T. Skauli, P. S. Kuo, K. L. Vodopyanov, T. J. Pinguet, O. Levi, L. A. Eyres, J. S. Harris, M. M. Fejer, B. Gerard, L. Becouarn, and E. Lallier, J. Appl. Phys. **94**, 6447 (2003).
[35] S. Adachi, J. Appl. Phys. **102**, 063502 (2007).
[36] Q. H. Song, L. Ge, J. Wiersig, J.-B. Shim, J. Unterhinninghofen, A. Eberspächer, W. Fang, G. S. Solomon, and H. Cao, Phys. Rev. A **84**, 063843 (2011).
[37] H. E. Türeci, A. D. Stone, and B. Collier, Phys. Rev. A **74**, 043822 (2006).
[38] L. Ge, Y. D. Chong, and A. D. Stone, Phys. Rev. A **82**, 063824 (2010).

Reuse of AIP Publishing content is subject to the terms at: https://publishing.aip.org/authors/rights-and-permissions. IP: 130.132.173.84 On: Fri, 05 Feb 2016 20:30:23